

LA-7855-MS

Informal Report

c.3

CIC-14 REPORT COLLECTION

**REPRODUCTION
COPY**

Neutron Scattering Cross Sections for ^{242}Pu

University of California

LOS ALAMOS NATIONAL LABORATORY



3 9338 00209 1956



LOS ALAMOS SCIENTIFIC LABORATORY

Post Office Box 1663 Los Alamos, New Mexico 87545

An Affirmative Action/Equal Opportunity Employer

This report was prepared as an account of work sponsored by the United States Government. Neither the United States nor the United States Department of Energy, nor any of their employees, nor any of their contractors, subcontractors, or their employees, makes any warranty, express or implied, or assumes any legal liability or responsibility for the accuracy, completeness, or usefulness of any information, apparatus, product, or process disclosed, or represents that its use would not infringe privately owned rights.

LA-7855-MS
Informal Report
UC-34c
Issued: October 1979

Neutron Scattering Cross Sections for ^{242}Pu

D. M. Drake
M. Drosch*
P. Lisowski
L. Veesser



*Institute for Experimental Physics, Strudlhofg. 4, A-1090, Wien, Austria.



NEUTRON SCATTERING CROSS SECTIONS FOR ^{242}Pu

by

D. M. Drake, M. Drosig, P. Lisowski, and L. Veaser

ABSTRACT

Differential cross sections for neutron scattering from ^{242}Pu are reported for 10 angles at each of three incident neutron energies: 0.57, 1.0, and 1.5 MeV.

I. INTRODUCTION

We measured neutron scattering cross sections of ^{242}Pu for incident neutrons of 0.57, 1.0, and 1.5 MeV and 10 angles. These cross sections can be used to determine optical model parameters that subsequently can be employed to calculate neutron scattering from ^{242}Pu over a large energy range.

II. EXPERIMENTAL ARRANGEMENT

Time-of-flight (TOF) techniques that incorporate a pulsed neutron beam and a fast liquid scintillator were used to measure the emitted neutron energy spectra. Figure 1 shows the experimental arrangement.

A. Neutron Sources

Two different neutron-producing reactions were used as the sources of monoenergetic neutrons for this experiment: $^7\text{Li}(p,n)^7\text{Be}$ for 0.57- and 1.0-MeV $^7\text{Li}(p,n)$ neutrons and $^3\text{H}(p,n)^3\text{He}$ for 1.5-MeV neutrons. The pulsed proton beam (1-ns time width at a 2-MHz repetition rate) was produced by the Los Alamos Scientific Laboratory (LASL) vertical Van de Graaff generator. For 2-MeV protons, the lithium target was a 25-keV-thick deposit of ^7LiF on a gold disk. The tritium target was a 20-mm-long gas cell with a 5.3-mg/cm^2 molybdenum entrance window and a gold beam stop. The energy spread of the neutrons from the gas cell was about 50 keV.

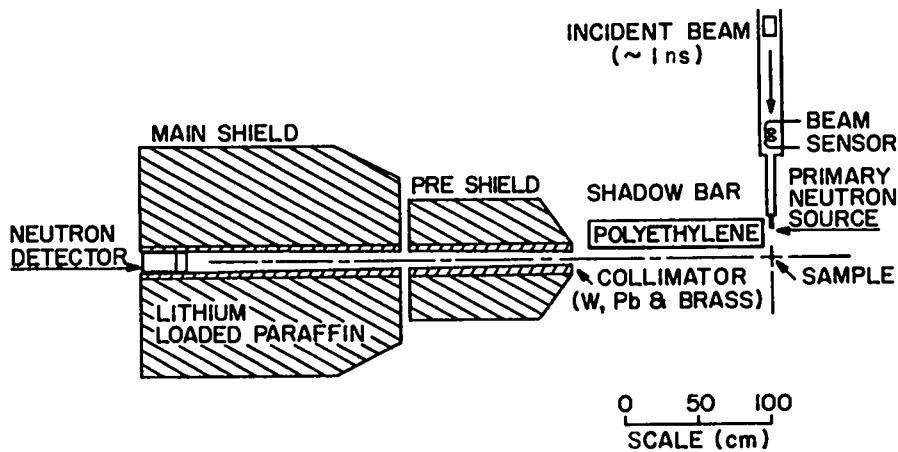


Fig. 1. Experimental arrangement for fast neutron TOF measurements.

B. ^{242}Pu Sample

The plutonium sample, located 100 mm in front of the neutron target, consisted of six 6.4-mm-diam and 15-mm-high cylinders, with a total mass of 47.25 g. These cylinders were placed in contact with the inner surface of a thin cylindrical 19-mm-i.d. aluminum can. This arrangement was chosen so that the sample would resemble a hollow right circular cylinder. During the experiment, the sample was rotated ~ 1 rpm around its vertical axis to eliminate any angular dependence of the scattering caused by this unusual sample configuration. An empty aluminum can with the same dimensions as the one that held the plutonium was used to correct for neutrons scattered from aluminum.

C. Neutron Detector

Neutrons that emerged from the ^{242}Pu sample were detected with an NE 213 liquid scintillator positioned in a massive shield of tungsten and lithium-loaded paraffin. A standard pulse-shape discrimination circuit was used to reject gamma-ray pulses. The liquid scintillator was coupled directly onto the face of an RCA 8854 photomultiplier tube. A large polyethylene shadow bar shielded the detector from the target's direct neutron flux. The distance between the sample and the center of the scintillator was 2.28 m. The reaction angle was changed by rotating the detector and shield around the center of the sample.

Two detector biases were used throughout the experiment. The higher bias was set at the pulse height minimum between the 26- and 60-keV ^{241}Am gamma rays as shown in Fig. 2. The TOF spectra of pulses between the higher bias and the

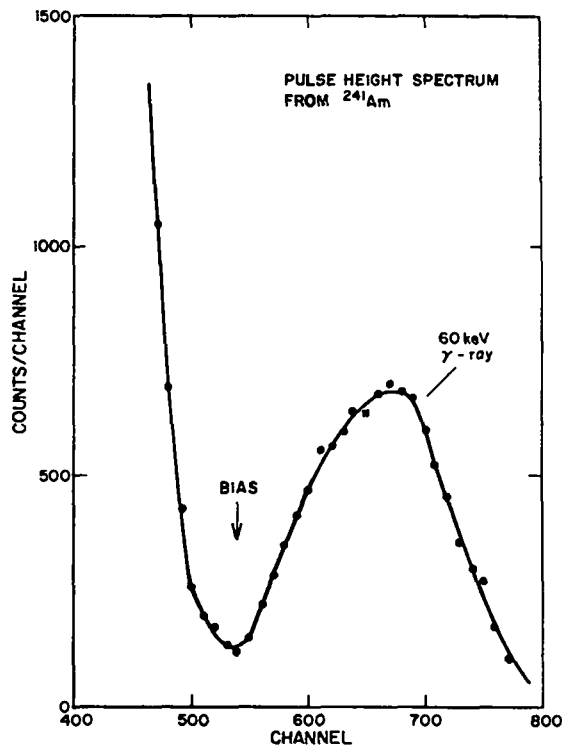


Fig. 2. The pulse height spectrum of ^{241}Am gamma rays in the NE 213 detector, showing the bias position.

lower bias were not useful because few neutrons of interest give rise to pulses in this energy range. We therefore analyzed only data for the higher bias.

A small liquid scintillator detector, located 5 m from the target at 0° , monitored neutrons by TOF and was used, with a measurement of the target current, to normalize the measurements.

III. DATA COLLECTION AND ANALYSIS

The TOF spectra were obtained from an EG&G TDC-100 time digitizer whose start and stop inputs were derived from the detector anode pulse and a beam sensor located just in front of the target.

The TOF spectrum of the empty aluminum can was used to correct for scattering from the aluminum can that held the plutonium. Before subtraction, however, the spectrum of the empty can had to be modified to account for neutron attenuation in the plutonium. After subtraction, the net spectrum always contained an excess number of counts because of the natural radioactivity of the plutonium sample. This constant background, which was determined from a region of the spectrum where only time-independent counts should occur, was subtracted from the raw spectrum. These corrections have already been applied to the 55° TOF spectrum shown in Fig. 3 for incident neutrons of 0.57 MeV.

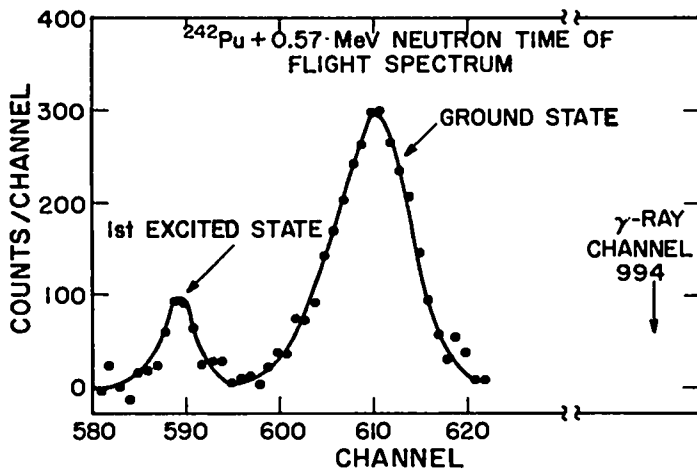


Fig. 3. TOF spectrum for 0.57-MeV incident neutrons. Backgrounds from the empty aluminum can and the natural radioactivity of the sample have been subtracted.

Differential cross sections for the separable peaks can be computed in two ways. The first method uses a zero-degree measurement of the neutron flux and the equation

$$\frac{d\sigma}{d\Omega} = \frac{(\text{Pu Counts}) (R^2)}{(\text{Pu nuclei}) (\text{Counts at } 0^\circ)} \left(\frac{d}{d_0}\right)^2 \frac{\epsilon(E_0)}{\epsilon(E_1)} M, \quad (1)$$

in which

$\frac{d\sigma}{d\Omega}$ = the differential cross section for the peak of interest,

Pu Counts = the number of counts in the peak of interest from Pu,

Pu Nuclei = the number of ^{242}Pu nuclei in the sample,

R = the harmonic mean of the distance from the target to the sample,

(Counts at 0°) = the number of counts in the peak with the detector at 0° ,

$\frac{d}{d_0}$ = the ratio of the distances sample to detector and target to detector,

$\frac{\epsilon(E_0)}{\epsilon(E_1)}$ = the ratio of the neutron detection efficiencies for source neutrons of energy E_0 and scattered neutrons of energy E_1 , and

M = the multiple scattering correction.

The second method relates the plutonium differential cross section to the well-known cross section of neutron scattering by hydrogen through the equation

$$\frac{d\sigma}{d\Omega} = \frac{(\text{Pu Counts})(\text{H Nuclei})}{(\text{H Counts})(\text{Pu Nuclei})} \frac{\epsilon(E_H)}{\epsilon(E_{Pu})} M \frac{d\sigma}{d\Omega} (np) , \quad (2)$$

in which

H Counts = the number of counts in the peak of neutrons scattered by hydrogen ,

H Nuclei = the number of hydrogen nuclei in the hydrogen sample ,

$\frac{d\sigma}{d\Omega} (np)$ = the differential cross section for np scattering, and

$\frac{\epsilon(E_H)}{\epsilon(E_{Pu})}$ = the ratio of neutron detection efficiencies for energies corresponding to neutrons scattered from hydrogen and neutrons scattered from plutonium.

We used both methods to compute cross sections for incident neutron energies of 0.57 and 1.0 MeV, and the results agree to within 4% for 0.57 MeV and 2% for 1.0 MeV. For incident neutrons of 1.5 MeV, only Eq. (2) was used.

The relative efficiency of this detector is well known.¹ However, because the energies of the scattered neutrons are only slightly less than the energy of neutrons in the incident beam, only a small segment of the efficiency curve is needed.

Attenuation and multiple scattering corrections for elastically scattered neutrons were obtained from neutron transport calculations made with the LASL Monte Carlo code MCNP.² Attenuation accounts for a relatively constant 30% correction, whereas the multiple scattering correction is angle dependent at ~2% at 20° and 33% in the cross section minimum near 70° for 1.5-MeV incident neutrons. Because the inelastic cross sections are almost isotropic, we used a procedure developed by Cranberg and Levin³ for heavy nuclei to calculate multiple scattering and attenuation corrections for differential inelastic scattering. This correction can be applied only to the angle-integrated cross sections for elastic scattering because the multiple scattering is angle dependent. We made these calculations also, and the corrections for the angle-integrated elastic scattering cross section agreed to within 4% of the Monte Carlo correction.

IV. RESULTS AND DISCUSSION

Results of these measurements are shown in Figs. 4 through 6 and are listed in Table I. The errors listed in Table I are statistical in origin. Additional systematic errors were estimated to be 11, 13, and 12% for the 0.57-, 1.0-, and 1.5-MeV data, respectively, and arise from uncertainties in normalization, efficiency, multiple scattering, and attenuation estimates. Because some of these errors vary with different experimental conditions, they are only approximate. Because few experimental results exist for ^{242}Pu , comparisons are made with nearby elements having similar properties and an evaluation by Madland and Young⁴.

A. Incident Neutrons of 0.57 MeV

Angle integration of the elastic and inelastic ($E^* = 45$ keV) cross sections (Fig. 4) results in cross sections of 5.9 and 1.3 b, respectively. The elastic cross section agrees with that measured by Cranberg and Levin⁵ for ^{238}U at 0.55 MeV but is nearly 0.4 b higher than the measurement by Smith et al.⁶ for ^{240}Pu . The inelastic cross section is about 10% lower than the measured value for ^{238}U in the 45-keV state. Summation of partial cross sections, $\sigma_{e1} = 5.9$ b, $\sigma_{in} = 1.3 + 0.30$ b (Ref. 5), $\sigma_f = 0.4$ b (Ref. 7), and $\sigma_{n,\gamma} = 0.1$ b results in a total cross section of 8.0 b. This is also ~ 0.5 b higher than the measured value for ^{240}Pu but agrees with the values in Brookhaven National Laboratory (BNL) report for ^{238}U . The evaluated total cross section (Ref. 4) is higher than our measurement due primarily to 0.5 b more elastic scattering.

B. Incident Neutrons of 1 MeV

Angle integration of the elastic and inelastic ($E^* = 0.045, 0.148$ MeV) differential cross sections shown in Fig. 5 results in cross sections of 4.3 b for elastic scattering, 1.10 b for inelastic scattering from the 0.045-MeV state and 0.42 ± 0.10 b for scattering from the 0.148-MeV state. Summation of these partial cross sections with 1.4 b for (n,f) gives 7.3 b for the total section, which agrees with values of 7.5 b (Ref. 6) for ^{240}Pu , 6.7 ± 0.6 b of Cranberg and Levin³, 7.2 b (Ref. 7) for ^{238}U , and 7.2 b from the evaluation (Ref. 4). The total elastic cross section also agrees with these references. One would expect that the inelastic cross sections and the compound elastic portion of the elastic would be smaller than those for ^{238}Pu because the fission channel is completely open for ^{242}Pu . The 1-MeV 90° cross sections reported by Beghian et al.⁸ for ^{238}U agree with the present data for the inelastic scattering but not for the elastically scattered neutrons.

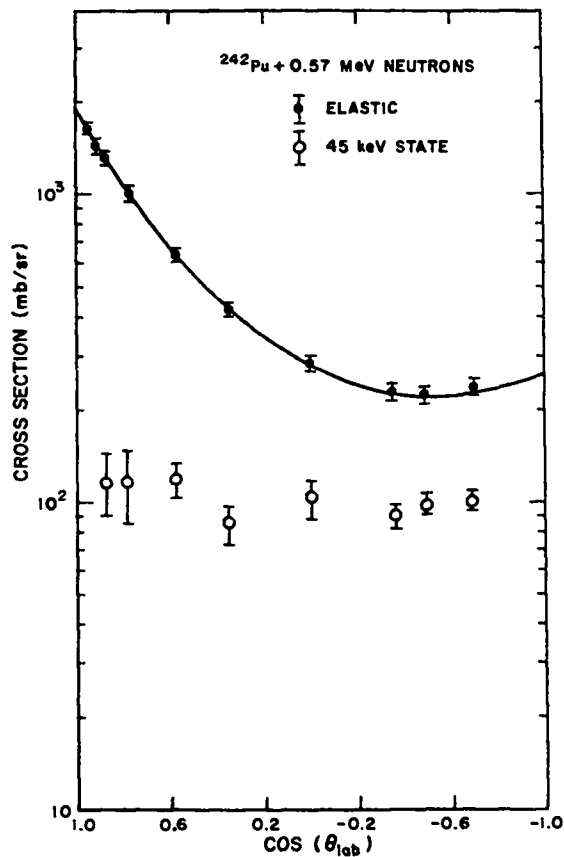


Fig. 4.

Differential cross sections for the ground and first excited states of $^{242}\text{Pu} + n$ for 0.57-MeV incident neutron energy.

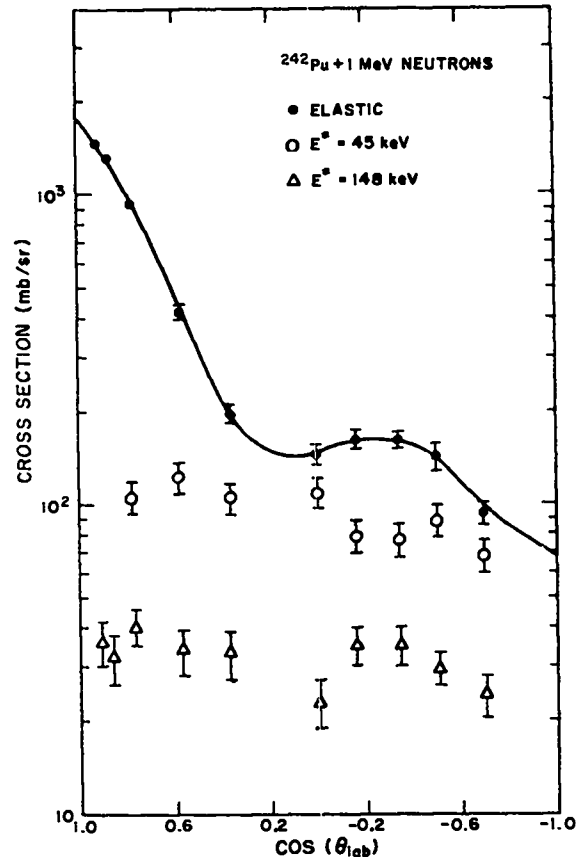


Fig. 5.

Differential cross sections for the ground, first, and second excited states of $^{242}\text{Pu} + n$ for 1.0-MeV incident energy.

C. Incident Neutrons of 1.5 MeV

It was impossible for us to separate elastically scattered neutrons from those inelastically scattered by low-lying excited states, so we analyzed the observed scattering as if it were one state. From these differential cross sections, we subtracted the 46 mb/sr that were estimated as the isotropic differential cross sections of the first two excited states.

As shown in Fig. 7, two other peaks are observed in the TOF spectra that correspond to excited states near 0.8 MeV and 1.0 MeV, where another rotational band based on a 1^- state begins and a second 0^+ state occurs. Each of these peaks has a cross section of 0.31 ± 0.10 b. Summation of the partial cross sections, $\sigma_e = 3.94$ b, $\sigma_i = 0.6 + 0.6 = 1.2$ b, and $\sigma_f = 1.4$ b, gives 6.6 b for a total cross section. This also agrees with total cross sections of 7.0 b for ^{238}Pu (Ref. 7), ^{240}Pu (Ref. 6), and ^{242}Pu (Ref. 4), although we may have missed some weaker inelastic states in our summation.

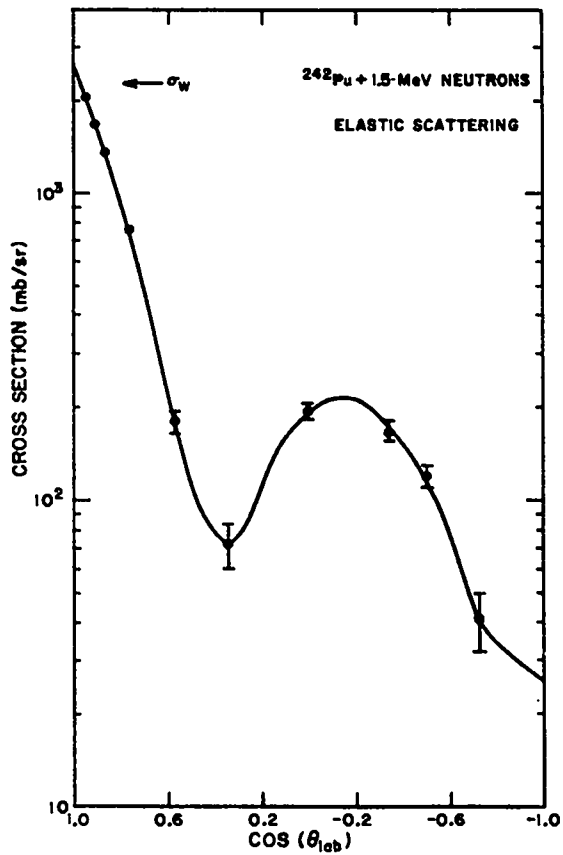


Fig. 6. Differential cross sections for the ground state of $^{242}\text{Pu} + n$ at 1.5 MeV-incident energy.

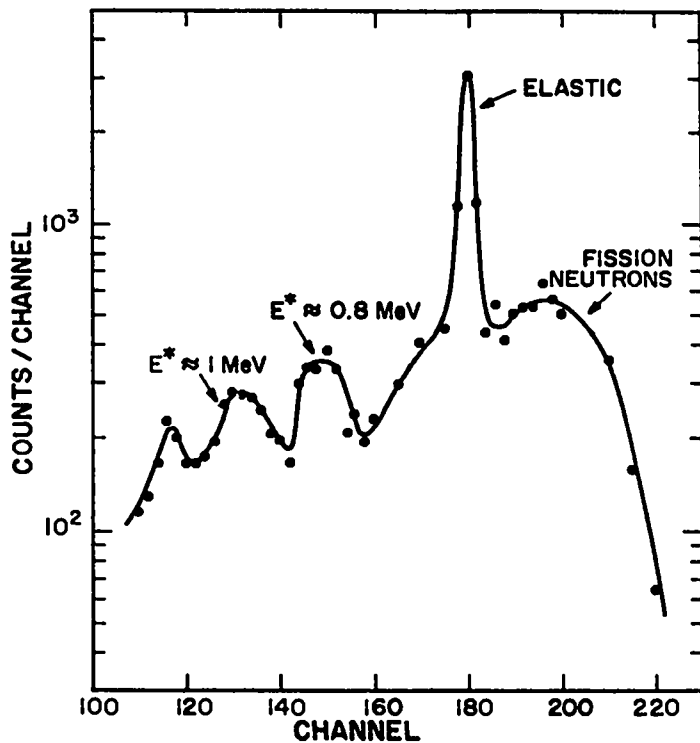


Fig. 7. Neutron TOF spectrum for 1.5-MeV incident neutrons interacting with ^{242}Pu . The elastic peak includes the first and second excited states. This spectrum also shows two peaks at 0.8- and 1.0-MeV excitation energy.

TABLE I
LABORATORY CROSS SECTIONS FOR NEUTRON SCATTERING FROM ^{242}Pu

θ_{Lab} (deg)	$d\sigma/d\Omega$ (mb/sr) for Incident Energy = 0.57 (MeV)		$d\sigma/d\Omega$ (mb/sr) for Incident Energy = 1.0 (MeV)			$d\sigma/d\Omega$ (mb/sr) Incident Energy = 1.5 (MeV)
	Elastic	45 keV	Elastic	45 keV	148 keV	Elastic
20	1615 \pm 80					2069 \pm 33
25	1423 \pm 75		1496 \pm 23	85 \pm 25	36 \pm 6	1645 \pm 28
30	1318 \pm 65	117 \pm 28	1315 \pm 14	77 \pm 25	32 \pm 6	1340 \pm 22
40	1003 \pm 50	117 \pm 33	934 \pm 33	105 \pm 12	41 \pm 5	670 \pm 17
55	673 \pm 34	119 \pm 14	418 \pm 18	123 \pm 14	34 \pm 5	180 \pm 13
70	422 \pm -1	84 \pm 12	198 \pm 14	104 \pm 12	33 \pm 6	73 \pm 13
90	284 \pm 16	103 \pm 15	145 \pm 11	109 \pm 12	23 \pm 4	195 \pm 9
100			162 \pm 11	78 \pm 9	35 \pm 5	
110	229 \pm 14	90 \pm 8	162 \pm 10	77 \pm 9	35 \pm 5	166 \pm 10
120	225 \pm 16	98 \pm 7	143 \pm 15	88 \pm 10	29 \pm 4	119 \pm 10
134.3	239 \pm 10	102 \pm 7	93 \pm 9	68 \pm 8	24 \pm 4	41 \pm 9
Angle Integrated $\sigma(b)$	5.91 \pm 0.70	1.28 \pm 0.18	4.3 \pm 0.5	1.19 \pm 0.17	0.42 \pm 0.08	3.94 \pm 0.5

REFERENCES

1. M. Drosog, D. M. Drake, and P. Lisowski, to be published in Nucl. Inst. & Meth.
2. E. D. Cashwell, J. R. Neergaard, W. M. Taylor, and G. D. Turner, "MCN: A Neutron Monte Carlo Code," Los Alamos Scientific Laboratory report LA-4751 (January 1972).
3. L. Cranberg and J. S. Levin, "Neutron Scattering by ^{235}U , ^{239}Pu , and ^{238}U ," Los Alamos Scientific Laboratory report LA-2177 (January 1959).
4. D. G. Madland and P. G. Young, "Evaluation of $n + ^{242}\text{Pu}$ Reactions from 10 KeV to 20 MeV," Los Alamos Scientific report LA-7533-MS (October 1978).
5. L. Cranberg and J. S. Levin, "Inelastic Neutron Scattering by ^{238}U ," Phys. Rev. 109, 2063-2068 (1958).
6. A. B. Smith, P. Lambropoulos, and J. F. Whalen, "Fast Neutron Total and Scattering Cross Sections of ^{240}Pu ," Nucl. Sci. Eng. 47, 19-28 (1972).
7. D. I. Garber and R. R. Kinsey, "Neutron Cross Sections, Volume II, Curves," Brookhaven National Laboratory report 325, 3rd Ed., Vol. II (1976).
8. L. E. Beghian, G. H. R. Kegel, T. V. Marcella, B. K. Barns, G. P. Couchell, J. J. Egan, A. Mittler, D. J. Pullen, and W. A. Schier, "Neutron Scattering Cross Sections of Uranium-238," Nucl. Sci. Eng. 69, 191-110 (1979).

Printed in the United States of America. Available from
National Technical Information Service
US Department of Commerce
5285 Port Royal Road
Springfield, VA 22161

Microfiche \$3.00

001-025	4.00	126-150	7.25	251-275	10.75	376-400	13.00	501-525	15.25
026-050	4.50	151-175	8.00	276-300	11.00	401-425	13.25	526-550	15.50
051-075	5.25	176-200	9.00	301-325	11.75	426-450	14.00	551-575	16.25
076-100	6.00	201-225	9.25	326-350	12.00	451-475	14.50	576-600	16.50
101-125	6.50	226-250	9.50	351-375	12.50	476-500	15.00	601-625	

Note: Add \$2.50 for each additional 100-page increment from 601 pages up.